Observation of Cesium ($nD_{5/2}$+$6S_{1/2}$) Ultralong-Range Rydberg-Ground Molecules

Su-Ying Bai(白素英)[1], Jing-Xu Bai(白景旭)[1], Xiao-Xuan Han(韩小萱)[1], Yue-Chun Jiao(焦月春)[1,2], Jian-Ming Zhao(赵建明)[1,2*], and Suo-Tang Jia(贾锁堂)[1,2]

[1]*State Key Laboratory of Quantum Optics and Quantum Optics Devices, Institute of Laser Spectroscopy, Shanxi University, Taiyuan 030006, China*

[2]*Collaborative Innovation Center of Extreme Optics, Shanxi University, Taiyuan 030006, China*

(Received 14 September 2020; accepted 21 October 2020; published online)

Ultralong-range Cs_2 Rydberg-ground molecules ($nD_{5/2} + 6S_{1/2}F$) ($33 \leq n \leq 39$, $F = 3$ or 4) are investigated by a two-photon photo-association spectroscopy of an ultracold Cs gas. Two vibrational ground molecular spectra of triplet $^3\Sigma$ and hyperfine mixed singlet-triplet $^{1,3}\Sigma$ molecular states and their corresponding binding energies are attained. The experimental observations are simulated by an effective Hamiltonian including low energy electron scattering pseudopotentials, the spin-orbit interaction of the Rydberg atom, and the hyperfine interaction of the ground-state atom. The zero-energy singlet and triplet s-wave scattering lengths are extracted by comparing the experimental observations and calculations. Dependences of the measured binding energies on the effective principal quantum number, $n_{\rm eff} = n - \delta_D$ (δ_D is the quantum defect of Rydberg D state), yield the scaling of $n_{\rm eff}^{-5.60\pm0.16}(^3\Sigma, F = 3)$, $n_{\rm eff}^{-5.62\pm0.16}(^3\Sigma, F = 4)$ for deep triplet potential and $n_{\rm eff}^{-5.65\pm0.38}(^{1,3}\Sigma, F = 3)$, $n_{\rm eff}^{-6.19\pm0.14}(^{1,3}\Sigma, F = 4)$ for shallow mixed singlet-triplet potential well. The simulations of low-energy Rydberg electron scattering show agreement well with the experimental measurements.

PACS: 32.80.Ee, 33.20.−t, 34.20.Cf DOI: 10.1088/0256-307X/37/12/123201

Ultralong-range Rydberg-ground molecules, composed of a Rydberg state atom and one or more ground state atoms, have attracted considerable attention due to their permanent electric dipole moments,[1,2] which are unique for homonuclear molecules. These molecules arise from low-energy scattering between the Rydberg electron and ground-state atoms that located inside the Rydberg electron's wave function. This low energy scattering interaction[3,4] has been predicted by a new binding mechanism of molecules that create a novel type of Rydberg molecules, including the s-wave dominated trilobite[1] and p-wave dominated butterfly molecules.[5,6]

Rydberg-ground molecules were first predicted theoretically two decades ago[1] and then observed experimentally in ultracold rubidium gases.[7] Subsequently, several groups have reported the observations of the Rydberg-ground molecules with Rb $nP_{1/2,3/2}$[8] and $nD_{3/2,5/2}$[9−11] states, as well as with Cs $nS_{1/2}$,[2,12] $nP_{3/2}$[13] and $nD_{3/2,5/2}$.[14,15] Recently, a new approach to excite ion-pair states of ultracold Rydberg-ground molecules was proposed,[16] putting forward a new method to form heavy-Rydberg states.[17] Due to large size and permanent electric dipole moment, Rydberg-ground molecule becomes an ideal candidate for investigating the strong correlated many-body gases[18] and quantum information processing.[19−21]

In this work, we present experimental observations of Cs_2 ($nD_{5/2} + 6S_{1/2}F$), (n = 33–39), long-range Rydberg-ground molecules employing a two-photon photoassociation technique. Two molecular states coming from a triplet s-wave scattering interaction, $^3\Sigma$, and a mixed singlet-triplet s-wave scattering interaction, $^{1,3}\Sigma$, are observed. The dependences of binding energies of the vibrational ground state $^3\Sigma(v = 0)$ and $^{1,3}\Sigma(v = 0)$ on the principal quantum number are extracted by analyzing the photoassociation spectroscopies. The Fermi model is employed to calculate molecular potential energy curves (PECs) and vibrational energies, which show agreement well with the measurements.

The Rydberg-ground molecule is bound by the low energy electron scattering interaction between Rydberg electron and a ground atom. We first calculate the PECs and related vibrational energies. The scattering interaction between the Rydberg electron and the ground-state atom is described by Fermi pseudopotential[3,4] in which the ground state atom is considered as a point perturber. The scheme of scat-

Supported by the National Key R&D Program of China (Grant No. 2017YFA0304203), the National Natural Science Foundation of China (Grant Nos. 11434007, 61835007, 61675123, 61775124, and 11904215), Changjiang Scholars and Innovative Research Team in Universities of Ministry of Education of China (Grant No. IRT 17R70), and the 1331 Project.

*Corresponding author. Email: zhaojm@sxu.edu.cn

tering interaction is demonstrated in Fig. 1(a). The Rydberg electron (ground atom) sits at position $\boldsymbol{r}$ ($R\hat{\boldsymbol{z}}$) relative to the Cs^+ ionic core. $\hat{\boldsymbol{I}}_2$ is ground-state-atom nuclear spin, $\hat{\boldsymbol{S}}_1$ and $\hat{\boldsymbol{S}}_2$ are the electronic spins of the Rydberg and the ground-state atom, respectively. In the reference frame of the Rydberg ionic core, the scattering interaction is expressed as[4]

$$\hat{V}(\boldsymbol{r};R) = 2\pi a_{\rm s}(k)\delta^3(\boldsymbol{r}-R\hat{\boldsymbol{z}}) + 6\pi[a_{\rm p}(k)]^3\delta^3(\boldsymbol{r}-R\hat{\boldsymbol{z}})\overleftarrow{\nabla}\cdot\overrightarrow{\nabla}, \quad (1)$$

where $a_l(k)$ is energy-dependent scattering length with l the scattering partial-wave order and k the electron momentum of the Rydberg atom; $l = 0$ (1) displays s-wave (p-wave) scattering. The scattering length $a_l(k)$ is written as $a_l(k)^{2l+1} = -\tan\eta_l(k)/k^{2l+1}$ with $\eta_l(k)$ the scattering phase shifts.

The Hamiltonian of the system includes three terms,[22]

$$\hat{H}(\boldsymbol{r};R) = \hat{H}_0 + \sum_{i=\rm S,T}\hat{V}(\boldsymbol{r};R)\hat{P}(i) + A_{\rm HFS}\hat{\boldsymbol{S}}_2\cdot\hat{\boldsymbol{I}}_2. \quad (2)$$

The first term, $\hat{H}_0$, is the Hamiltonian of the Rydberg atom. The second term displays the scattering interactions, which sums over the spin-dependent singlet ($i = $ S) and triplet ($i = $ T) scattering channels, using the projection operators $\hat{P}(\rm T) = \hat{\boldsymbol{S}}_1\cdot\hat{\boldsymbol{S}}_2 + 3/4$, $\hat{P}(\rm S) = 1 - \hat{P}(\rm T)$. The last term represents the hyperfine interaction of the ground state atom with $A_{\rm HFS}$ hyperfine parameter.

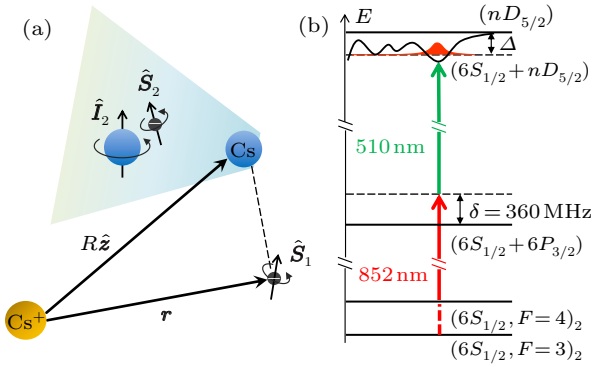

Fig. 1. (a) Schematic of the molecular system. The Rydberg electron with spin $\hat{\boldsymbol{S}}_1$ sits at position $\boldsymbol{r}$ relative to the ionic core. A cesium ground state atom is located at position $R\hat{\boldsymbol{z}}$ relative to the ionic core of the Rydberg atom. $\hat{\boldsymbol{S}}_2$ and $\hat{\boldsymbol{I}}_2$ are electronic and nuclear spins of the ground state atom, respectively. (b) Two-photon excitation diagram. First photon, 852 nm laser, drives $|6S_{1/2}, F=3\rangle$ or $|6S_{1/2}, F=4\rangle \rightarrow |6P_{3/2}, F'=5\rangle$ transition, while second photon, 510 nm laser, drives $|6P_{3/2}, F'=5\rangle \rightarrow |nD_{5/2}\rangle$ transition. The 852 nm laser frequency is blue shifted from the intermediate level $|6P_{3/2}, F'=5\rangle$ by 360 MHz using a double-pass acousto-optic modulator (AOM). The 510-nm frequency is scanned to red detuning from $nD_{5/2}$ Rydberg atomic line.

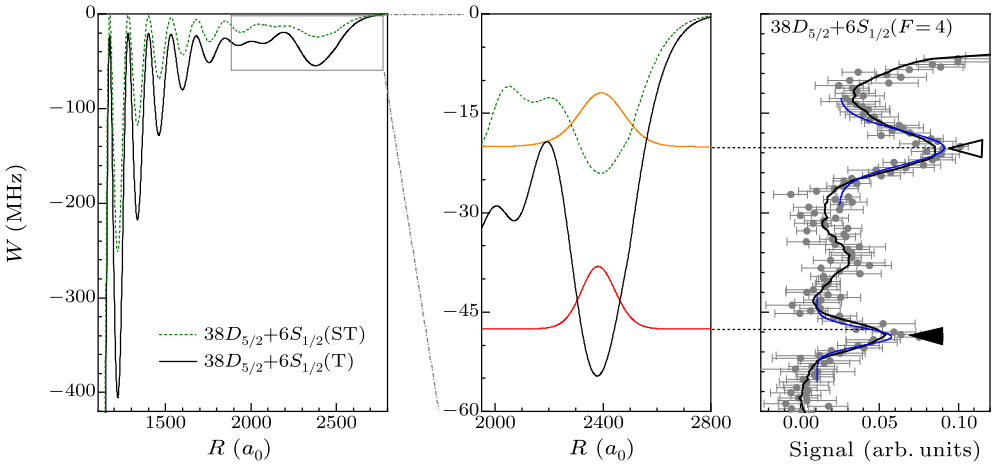

Fig. 2. Calculations of PECs and measured spectrum for the $38D_{5/2} + 6S_{1/2}(F = 4)$ Rydberg molecule related to the $38D_{5/2}$ atomic line. Left panel displays the calculated PECs of the $38D_{5/2} + 6S_{1/2}(F = 4)$ Rydberg molecule. The solid (dashed) line is the PECs formed mostly by triplet (mixed singlet-triplet) scattering for $6S_{1/2}F = 4$. The outmost potential wells marked with a square mainly arise from s-wave scattering and are enlarged in the middle panel. The red and yellow lines indicate the ground vibrational wave functions of $^3\Sigma$ and $^{1,3}\Sigma$ potentials, respectively. Right panel presents the measured spectrum for the $38D_{5/2} + 6S_{1/2}(F = 4)$ molecule. The triangles indicate two molecular signals and the black line displays smoothed average. We extract the binding energy of the molecular state by Gaussian fitting of the molecular peaks, as shown by the blue lines.

We diagonalize the Hamiltonian of Eq. (2) and attain adiabatic potential energy curves $W_{\rm ad}(R)$. The left panel of Fig. 2 presents the calculations of PECs of Rydberg molecules that are asymptotically connected with the atomic $38D_{5/2}$ state, with the ground-state atom being in $6S_{1/2}F = 4$ hyperfine level. It is seen that two PECs display outermost energy minimum of dozens of megahertz deep at $R \simeq 2400a_0$, marked with

a gray square and enlargement in the middle panel of Fig. 2, where the electron atom interaction is dominated by the s-wave scattering interaction forming a trilobite-type Rydberg molecule. The deep well potential (solid line) mostly arises from triplet s-wave scattering forming $^3\Sigma$ molecular state, whereas the shallow well potential (dashed line) mostly from hyperfine mixed singlet-triplet s-wave scattering forming $^{1,3}\Sigma$ state. In the middle panel of Fig. 2, we also plot the vibrational state and wave functions $\Psi_{\rm ad,v}(R)$, calculated with the molecular Hamiltonian theory. The deeper wells at $R \leq 1800a_0$ range mainly come from p-wave scattering interaction forming butterfly-type Rydberg molecules, which is beyond this work.

A Rydberg-ground molecular experiment is implemented in the crossed optical dipole trap (CODT) with the temperature $\sim$100 μK and peak density $\sim 10^{11}\,{\rm cm}^{-3}$, the detail of the experiment is described in our previous works.[15,23] The two-photon photoassociation method is employed to prepare the Rydberg-ground molecules, related excitation diagram as shown in Fig. 1(b). An 852 nm laser, driving a lower ground state transition $|6S_{1/2}, F = 4\rangle \rightarrow |6P_{3/2}, F' = 5\rangle$, and a 510 nm laser, driving an upper Rydberg transition $|6P_{3/2}, F' = 5\rangle \rightarrow |nD_{5/2}\rangle$, are overlapped in a counter propagating configuration. The frequencies of 852- and 510-nm excitation beams are stabilized to the same high-finesse Fabry–Pérot (FP) cavity with the linewidth less than 500 kHz. The 852-nm frequency is blue shifted from the intermediate level by $\delta = 360$ MHz with a double-pass acousto-optic modulator (AOM). The Rabi frequency of Rydberg excitation $\Omega = \Omega_{852}\Omega_{510}/2\delta \approx 2\pi \times 0.15$ MHz, with $\Omega_{852} = 2\pi \times 16.1$ MHz ($\Omega_{510} = 2\pi \times 6.8$ MHz) the Rabi frequency of the first (second) photon and $\delta = 360$ MHz the detuning of single photon. The 510-nm frequency is red detuned from the Rydberg atomic line by scanning the radio-frequency signal applied to the electro-optic modulator that is used to lock the laser to the FP cavity. The Rydberg molecules are created when the detuning from the atomic line matches the binding energy of the Rydberg-ground molecules. After two-photon excitation pulse, we apply a small electric field to extract the atomic (molecular) ions produced by the blackbody photoionization (Hornbeck–Molnar autoionization) to a microchannel plate (MCP) detector.

To attain the dependence of the Rydberg-ground molecular resonances on the hyperfine level, F-quantum number, of the ground state atom, we prepare the ground-state atoms in either the $F = 3$ or the $F = 4$ hyperfine level by turning the MOT repumping laser either off or on during the photo-association pulse sequence.

In the right panel of Fig. 2, we present a two-photon photoassociation spectrum of $38D_{5/2} + 6S_{1/2}(F = 4)$ Rydberg-ground molecules correlated with the $38D_{5/2}$ atomic line. The spectrum displays clearly two molecular peaks marked with triangles at red detuned side and well-resolved from each other and from the atomic line, allowing us to determine the binding energies of molecules with uncertainties less than 1 MHz. The binding energies are extracted by Gaussian fittings to the respective molecular peaks of measured spectra, see blue lines in the right panel of Fig. 2. The data are employed to obtain the dependence of the binding energy on the effective principal quantum number $n_{\rm eff}$ and to determine s-wave scattering lengths via comparison with model calculations.

We perform a series of measurements similar to Fig. 2 and obtain the two-photon photoassociation spectra of $nD_{5/2}+6S_{1/2}F$ for principal quantum number ($n = 33$–39) and hyperfine level $F = 3$ or 4 of the ground atom by varying the frequency of excitation laser. In Fig. 3, we present the typical photoassociation spectra for $n = 36$–39 range and the ground-state hyperfine levels $F = 3$ (left panel) and $F = 4$ (right panel), respectively. The measured spectra are averaged over ten independent measurements for decreasing systematic uncertainties, gray symbols and error bars show the original data, and the black lines display smoothed average. All spectra clearly display two dominant molecular peaks, marked with B (C), corresponding to the vibrational ground states of deep-well $^3\Sigma$ (shallow-well $^{1,3}\Sigma$) PECs, which mostly arise from s-wave scattering interaction, as mentioned above. Gaussian fittings to the respective molecular peaks yield the binding energies, see the blue lines in Fig. 3. For comparison, we also plot vertical solid (dashed) lines to represent the calculated binding energies of $^3\Sigma v = 0$ ($^{1,3}\Sigma v = 0$) states. It is seen that the measurements of the binding energy agree with the calculations. For instance, the measured binding energy is 48.2±0.5 MHz (19.7±0.5 MHz) for the $^3\Sigma$ ($^{1,3}\Sigma$) state of the $38D_{5/2} + 6S_{1/2}F = 4$ molecule, while the calculated binding energy is 47.6 MHz (20.1 MHz), corresponding deviation of 1.3% (2%). For molecular spectra of $nD_{5/2} + 6S_{1/2}F$ ($n = 33$–39, $F = 3$ or 4), the averaged deviation between measurements and calculations is 2.8%.

For attaining $n_{\rm eff}$ dependence of the binding energy ($n_{\rm eff} = n - \delta_D$, with δ_D quantum defect of Rydberg D state), we plot measurements of the binding energies of $nD_{5/2} + 6S_{1/2}$ molecules as a function of the principal quantum number for ground hyperfine level $F = 3$ in Fig. 4(a) and $F = 4$ in Fig. 4(b). For comparison, we also present the calculations of the binding energies in Fig. 4, showing a good agreement with the measurements. We use formula $y = an_{\rm eff}^b$ (with a and b being the fitting parameters) to fit the

data of Fig. 4 and obtain scaling laws, see the dashed red (measurement) and solid black (theory) lines in Fig. 4. A closer look further reveals that the exponents b are about -5.60, related scalings of measurements are $n_{\rm eff}^{-5.60\pm0.16}({}^3\Sigma, F=3)$, $n_{\rm eff}^{-5.62\pm0.16}({}^3\Sigma, F=4)$ for deep triplet potential and $n_{\rm eff}^{-5.65\pm0.38}({}^{1,3}\Sigma, F=3)$, $n_{\rm eff}^{-6.19\pm0.14}({}^{1,3}\Sigma, F=4)$ for shallow hyperfine mixed singlet-triplet potential well, respectively. Measurements of scaling b agree with the calculations, as displayed in Fig. 4, except the mixed ${}^{1,3}\Sigma, F=4$ potential, see detailed discussion in the following.

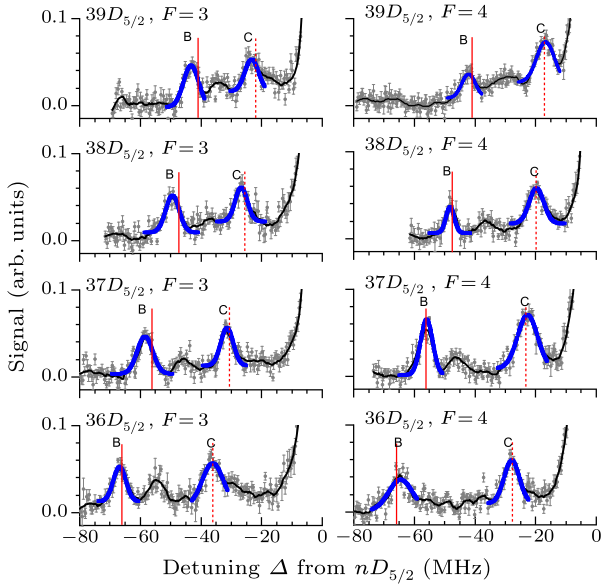

Fig. 3. Measurements of two-photon photoassociation spectra of $nD_{5/2}+6S_{1/2}(F=3)$ (left panel) and $nD_{5/2}+6S_{1/2}(F=4)$ (right panel) Rydberg-ground molecules with $n=36$–39. Peaks B and C indicate the vibrational ground molecular signals formed mainly by triplet (${}^3\Sigma$) and hyperfine-mixed singlet-triplet (${}^{1,3}\Sigma$) potentials, respectively. The vertical solid (dashed) red lines display the calculated ground vibrational levels of triplet (mixed) molecular states. The positions of triplet molecular signals are nearly the same for $F=3$ and $F=4$, while the positions of mixed molecular signals are deeper for $F=3$ than $F=4$.

It is noted that a procedure similar to the one described in Refs. [11,15] is employed to reproduce the binding energies of calculations. In the nonrelativistic approach, we use finite-range model potentials for the low-energy electron scattering provided in Ref. [24]. The s-wave singlet and triplet scattering wave-functions of the electron are integrated numerically and evaluated at a distance of $1000a_0$ from the perturber to determine the scattering lengths $a_{\rm s}^S(k)$ and $a_{\rm s}^T(k)$. To achieve agreement between experiment and theory it is necessary to fine-tune the s-wave scattering-length functions, $a_{\rm s}^S(k)$ and $a_{\rm s}^T(k)$, by phase-shifting the wave-function of the scattered electron by a small amount. The shifts of the scattered-electron wave-function are parameterized by the zero-energy scattering lengths, $a_{\rm s}^S(k=0)$ and $a_{\rm s}^T(k=0)$. Comparing with the measurements of Fig. 4 for all n in this work, we find average values of zero-energy scattering length $a_{\rm s}^S(k=0)=-1.92a_0$ and $a_{\rm s}^T(k=0)=-19.16a_0$, respectively. In our model, because the p-wave scattering has a relatively small effect on the PECs over the range of the outermost potentials, we use p-wave scattering-length functions $a_{\rm p}^S(k)$ and $a_{\rm p}^T(k)$ from Ref. [24] without further adjustment. Once the PECs are known, the vibrational wave functions, see the middle panel of Fig. 2, and the corresponding energies of vibrational resonances are obtained using the molecular Hamiltonian theory, as displayed in Fig. 4.

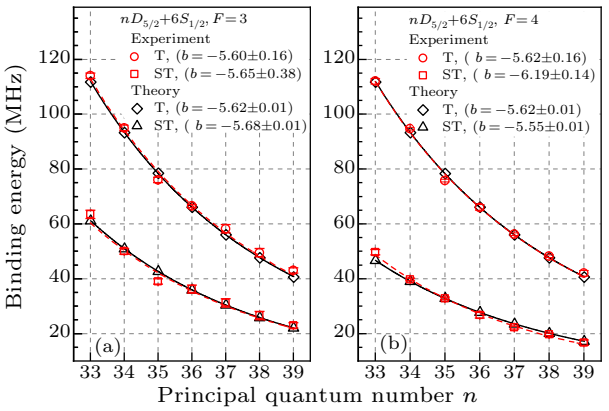

Fig. 4. Measurements (red symbols) and calculations (black symbols) of binding energies of Rydberg-ground molecules $nD_{5/2}+6S_{1/2}(F=3,4)$ for triplet ${}^3\Sigma(v=0)$ and hyperfine mixed singlet-triplet ${}^{1,3}\Sigma(v=0)$ ground vibrational states, (a) for ground hyperfine level $F=3$ and (b) for $F=4$. The experimental binding energies are extracted from Gaussian fittings to the molecular peaks of photo-association spectra of Fig. 3. Dashed red (solid black) lines display fittings to the experimental (calculated) binding energies using formula $y=an_{\rm eff}^b$, with fit parameters a and b.

From Figs. 3 and 4, we find that the positions or the binding energies of triplet molecular states are almost the same for ground hyperfine level $F=3$ and $F=4$, which means that the binding energies of the ${}^3\Sigma v=0$ molecular states do not significantly depend on F, over the entire range of n-values studied. This is due to fact that the binding energies measured for the ground states in the outermost wells in the ${}^3\Sigma$ PECs are almost unaffected by the hyperfine structure of the ground-state atom. In contrast, the binding energies measured for the ground states in the outermost wells of the mixed ${}^{1,3}\Sigma$ PECs depend on whether the ground-state atom is in its lower or upper hyperfine state ($F=3$ or 4), as described in Refs. [13,22]. Furthermore, we find that the binding energies of the ${}^{1,3}\Sigma v=0$ states for $F=4$ are always less than those for $F=3$, with the difference gradually decreasing from about 13 MHz at $n=33$ to about 6 MHz at $n=39$.

A close inspection of Fig. 4 reveals the good agreement between measured and calculated binding energies for all types of molecular PECs over large n range here. The exponents b also show good agreements, with the exception of the most weakly-bound case, mixed $^{1,3}\Sigma$ state of the $nD_{5/2} + 6S_{1/2}F = 4$ molecule. We attribute this disagreement to the fact that the most weakly bound states are the hardest case to measure, as the molecular resonances are the closest to the atomic lines with the smallest shifts, hence experimental uncertainties have the greatest effect. For instance, $nD_{5/2} + 6S_{1/2}F = 4$ molecular spectra in the right panel of Fig. 3, the $^{1,3}\Sigma$ molecular signals are closer to atomic line than the other molecular states. Furthermore, the vibrational wavefunctions of the most weakly-bound states extend the furthest towards small internuclear separations, where p-wave scattering may become important.

In summary, we have observed $nD_{5/2} + 6S_{1/2}Cs_2$ Rydberg-ground molecules involved ground-state hyperfine structure. The measurements of the binding energies both for deep triplet $^3\Sigma(v = 0)$ and shallow mixed $^{1,3}\Sigma(v = 0)$ molecular vibrational state agree well with the calculations with low-energy electron scattering theory for the n range used here. The hyperfine levels of the ground state atom are found to have a negligible effect on triplet $^3\Sigma(v = 0)$ potential well and the corresponding vibrational bind energy, but would modify the mixed $^{1,3}\Sigma$ potential well of Rydberg-ground molecules. The allometric fits to measurements and calculations of binding energy yield scaling laws with exponents b, showing a good agreement between the experiment and theory and closer to the previous works n^{-6} scaling of ^{87}Rb $nD + 5S$ molecules in reference.[9] The method used here can be used to prepare the Rydberg-ground state molecules with different angular moment states such as Cs $nP + 6S$[13] and $nS + 6S$[2,12] molecules and different atoms such as Rb $nD + 5S$[11] and Sr_2 Rydberg molecule.[25] In future, we will further investigate the interaction between the Rydberg molecule and an external field due to huge permanent dipole moment of the Rydberg-ground molecule.

References

[1] Greene C H, Dickinson A S and Sadeghpour H R 2000 *Phys. Rev. Lett.* **85** 2458
[2] Booth D, Rittenhouse S T, Yang J, Sadeghpour H R and Shaffer J P 2015 *Science* **348** 6230
[3] Fermi E 1934 *Nuovo Cimento* **11** 157
[4] Omont A 1977 *J. Phys. France* **38** 1343
[5] Hamilton E L, Greene C H and Sadeghpour H R 2002 *J. Phys. B: At. Mol. Opt. Phys.* **35** L199
[6] Chibisov M I, Khuskivadze A A and Fabrikant I I 2002 *J. Phys. B: At. Mol. Opt. Phys.* **35** L193
[7] Bendkowsky V, Butscher V, Nipper J, Shaffer J P, Löw R and Pfau T 2009 *Nature* **458** 1005
[8] Bellos M A, Carollo R, Banerjee J, Eyler E E, Gould P L and Stwalley W C 2013 *Phys. Rev. Lett.* **111** 053001
[9] Anderson D A, Miller S A and Raithel G 2014 *Phys. Rev. Lett.* **112** 163201
[10] Krupp A T, Gaj A, Balewski J B, Ilzhöfer P, Hofferberth S, Löw R, Pfau T, Kurz M and Schmelcher P 2014 *Phys. Rev. Lett.* **112** 143008
[11] Maclennan J L, Chen Y J and Raithel G 2019 *Phys. Rev. A* **99** 033407
[12] Tallant J, Rittenhouse S T, Booth D, Sadeghpour H R and Shaffer J P 2012 *Phys. Rev. Lett.* **109** 173202
[13] Saßmannshausen H, Merkt F and Deiglmayr J 2015 *Phys. Rev. Lett.* **114** 133201
[14] Fey C, Yang J, Rittenhouse S T, Munkes F, Baluktsian M, Schmelcher P, Sadeghpour H R and Shaffer J P 2019 *Phys. Rev. Lett.* **122** 103001
[15] Bai S, Han X, Bai J, Jiao Y, Wang H, Zhao J and Jia S 2020 *J. Chem. Phys.* **152** 084302
[16] Peper M and Deiglmayr J 2020 *J. Phys. B: At. Mol. Opt. Phys.* **53** 064001
[17] Reinhold E and Ubachs W 2005 *Mol. Phys.* **103** 1329
[18] Weimer H, Müller M, Lesanovsky I, Zoller P and Büchler H P 2010 *Nat. Phys.* **6** 382
[19] Lukin M D, Fleischhauer M, Cote R, Duan L M, Jaksch D, Cirac J I and Zoller P 2001 *Phys. Rev. Lett.* **87** 037901
[20] DeMille D 2002 *Phys. Rev. Lett.* **88** 067901
[21] Rabl P, DeMille D, Doyle J M, Lukin M D, Schoelkopf R J and Zoller P 2006 *Phys. Rev. Lett.* **97** 033003
[22] Anderson D A, Miller S A and Raithel G 2014 *Phys. Rev. A* **90** 062518
[23] Han X X, Bai S Y, Jiao Y C, Hao L P, Xue Y M, Zhao J M, Jia S T and Raithel G 2018 *Phys. Rev. A* **97** 031403(R)
[24] Khuskivadze A A, Chibisov M I and Fabrikant I I 2002 *Phys. Rev. A.* **66** 042709
[25] DeSalvo B J, Aman J A, Dunning F B, Killian T C, Sadeghpour H R, Yoshida S and Burgdörfer J 2015 *Phys. Rev. A* **92** 031403(R)